Sound & Vibration 2026, 60(5), 4180.
doi: https://doi.org/10.59400/sv4180

Article

Audio signal approximation and fuzzy logic-based acoustic noise-risk assessment using Fourier–Dirichlet analysis and hyperbolic series representations

Yogeesh Nijalingappa[1,2,3,*], Asokan Vasudevan[3], Soon Eu Hui[3], Zetty Pakir Mastan[4], Choo Wou Onn[5], Mohammed Almakki[6]

[1] Department of Mathematics, Government First Grade College, Tumkur 572102, India
[2] Mathematics & Natural Sciences, Gulf University for Science & Technology, Hawalli 32093, Kuwait
[3] Faculty of Business and Communications, INTI International University, Nilai 71800, Malaysia
[4] Faculty of Engineering and Quantity Surveying, INTI International University, Nilai 71800, Malaysia
[5] International Relations and Collaborations Centre, INTI International University, Nilai 71800, Malaysia
[6] School of Engineering, Architecture and Interior Design, Amity University Dubai, Dubai P.O. Box 345019, United Arab Emirates
*** Corresponding author:** Yogeesh Nijalingappa, yogeesh.n@ka.gov.in

CITATION

Nijalingappa Y, Vasudevan A, Hui SE, et al. Audio signal approximation and fuzzy logic-based acoustic noise-risk assessment using Fourier–Dirichlet analysis and hyperbolic series representations. Sound & Vibration. 60(5): 4180. https://doi.org/10.59400/sv4180

ARTICLE INFO

Received: 21 March 2026
Revised: 15 April 2026
Accepted: 20 April 2026
Available online: 24 July 2026

Abstract: This paper presents an acoustics-oriented study that combines classical Fourier–Dirichlet signal approximation with a fuzzy logic-based noise-risk interpretation layer. The harmonic-analysis part revisits Fourier series for periodic and quasi-periodic audio waveforms under classical Dirichlet conditions and restates these conditions in a form that is practically checkable on sampled audio segments; no new convergence theorem is claimed. A complementary hyperbolic-series representation is used as an illustrative analytical tool for discussing compact representations of selected waveform classes. The applied contribution of the paper is a Mamdani fuzzy inference system that converts uncertain acoustic measurements into an interpretable Noise-Risk Index using A-weighted equivalent sound level, daily exposure duration, and source–receiver distance. The fuzzy model uses triangular/trapezoidal memberships, an interpretable rule base, min–max inference, and centroid defuzzification. To show the practical usefulness in sound and vibration practice, one waveform-reconstruction example and a twelve-scenario acoustic-risk dataset with regard to traffic, workshop, generator room, and public address contexts are reported in the study. The resulting fuzzy system generates a range of risk scores from 22 to 92, lying within the safe, caution, high, and critical level categories and depicts smooth transitions as we approach decision boundaries where a crisp threshold can often be challenging to decode. This work thus establishes Fourier analysis as the underlying level for acoustic signals and fuzzy inference as a decision-support level in the context of uncertainty-based exposure assessment. The current coupling is linear instead of feature-driven: the Fourier-based signal description forms the basis for exposure descriptors, and the fuzzy system processes these descriptors given uncertainty.

Keywords: Fourier series; Dirichlet conditions; audio signal approximation; hyperbolic series; fuzzy logic; acoustic noise-risk assessment; Mamdani fuzzy inference; harmonic analysis

1. Introduction

Fourier–Dirichlet analysis and theory play a crucial role in coding periodic signals as harmonic constituents, most notably for spectral characterization, tonal analysis, and waveform reconstruction in domains such as audio, vibration, and condition monitoring [1,2]. In practice, the acquired acoustic signals are subject to limited record length, background noise, and mild nonstationarity, which render the interpretation of truncated harmonic expansions nontrivial [3–5].

We are not here claiming anything resembling a new Fourier convergence theorem, nor do we mean to supplant linear algebra approaches like windowing or power-spectrum estimation. Rather, it bridges a more specialized gap: periodic or quasi-periodic acoustic waveforms are often mathematically articulated, while exposure-based decisions derived from measured sound levels always take place under uncertainty. The study as such combines a classical Fourier–Dirichlet description with respect to waveform approximation and non-parametric fuzzy inference through a Mamdani structure for uncertainty-aware acoustic noise-risk interpretation. By "directly checkable from measured audio," we refer to practical checks of finite extrema, finite discontinuities, and piecewise smoothness on a specified analysis interval; no separate numerical verification of Dirichlet conditions is in claim. Thus, unlike in the proposed fuzzy formulation where Fourier coefficients may be used as direct fuzzy inputs, the harmonic stage allows a physically founded signal description while at the same time reducing the grid size of, for example, L_{Aeq}, duration, and distance descriptors that can be interpreted directly from measurements.

Recent work has begun treating signal characterization, exposure assessment, and health-oriented noise evaluation as related but separate problems. Transport and vibroacoustic analysis reviews still highlight spectral/Fourier tools to describe measured signals [1, 2] while recent studies on sonic hazard and environmental noise assessment have been more direct about exposure metrics, urban-noise effects [6–8], and ground-measurement risk interpretation [9–12]. Uncertain acoustic observations have also been converted into interpretable nuisance or risk indicators through fuzzy and rule-based approaches [13, 14]. One of the things still less explicit in the literature is a paper making clear that it is keeping the descriptive signal-analysis layer separated from the uncertainty-aware decision layer, but nevertheless discussing them together in a single acoustics workflow.

1.1. Preliminaries

This subsection gives a brief overview on (i) Fourier–Dirichlet series representation, periodic signals, (ii) practical coefficient estimation from accumulated sampled data, and finally (iii) one fuzzy-logic layer only used for uncertainty-aware noise-risk interpretation. Harbensson: The term "signal" implies an acoustic signal that is measured in time, while we interpret harmonic content through frequency-domain coefficients. Instead of computing Fourier coefficients, the fuzzy component summarizes uncertainty regarding environmental noise exposure using standard measurable components, including sound level, exposure duration, and distance.

The fuzzy membership functions used in this study [15] allow for imprecision: each acoustically relevant input variable is assigned degrees of membership. The membership functions within the rule base use the Mamdani–Assilian approach [16] to establish a relationship between A-weighted equivalent sound level, exposure duration per day, distance between the source and receiver, and an output in terms of linguistic noise risk. The combination of antecedents is performed using the minimum operator, and the result of this aggregation is passed through the centroid defuzzification function in order to output a scalar score [17, 18].

1.1.1. Signal approximation and Fourier series

The process of signal approximation involves breaking a waveform down into simpler components. Fourier series and transforms are a classical method for approximating periodic signals as the sum of sinusoidal functions [19].

But $x(t)$ is a real-valued periodic signal with period T and fundamental angular frequency $\omega 0 = 2\pi/T$. Under the Dirichlet conditions, $x(t)$ has a Fourier series of the form:

$$x(t) = \frac{a_0}{2} + \sum\nolimits_{n=1}^{\infty} \left[a_n \cos\left(n\omega_0 t\right) + b_n \sin\left(n\omega_0 t\right)\right],$$

where the Fourier coefficients are the standard Fourier expansion, and coefficient formulas follow classical treatments of periodic signal analysis [19,20],

$$a_n = \frac{2}{T}\int_0^T x(t)\cos\left(n\omega_0 t\right) dt,\ b_n = \frac{2}{T}\int_0^T x(t)\sin\left(n\omega_0 t\right) dt.$$

Assuming that the signal *x[k]* is sampled, periodic with a period of T, discover how many samples (N) are in a period. Look what we can do—and those coefficients could be approximated using numerical quadrature or DFT relations [21,22].

1.1.2. Dirichlet conditions for sampled audio

In this paper, “Dirichlet conditions” only refer to the classical convergence conditions for Fourier series, not related to PDE Dirichlet problems. Over a period, the signal is assumed to be piecewise smooth, have finitely many extrema, and to have finitely many discontinuities so that the Fourier series converges in the classical pointwise sense [23,24].

1.1.3. Hyperbolic series identities

Hyperbolic-series expressions are used here as basic analytical forms, involving functions such as $sinh(x)$ and $cosh(x)$. Because hyperbolic functions can also be expressed in terms of exponentials, they serve as a useful alternative representation when describing certain coefficient patterns [25]:

$$sinh(x) = \frac{e^x - e^{-x}}{2},$$

$$cosh(x) = \frac{e^x + e^{-x}}{2}.$$

1.1.4. Fuzzy membership functions

Membership functions assign values in the range [0,1] to each point in the input space. In this study, the linguistic variables are A-weighted sound level, daily exposure duration, source–receiver distance, and Noise-Risk Index; triangular and trapezoidal membership functions are used for simplicity and interpretability. The triangular and trapezoidal membership-function forms used below are standard in fuzzy-system design [15,17].

$$\text{Low Membership Function: } \mu_{\text{Low}}(x) = \max\left(0, \min\left(\frac{5-x}{5}, 1\right)\right).$$

This function peaks at the lowest value and decreases linearly to zero as x increases.

$$\text{Medium Membership Function: } \mu_{\text{Medium}}(x) = \max\left(0, \min\left(\frac{x-2.5}{2.5}, \frac{7.5-x}{2.5}\right)\right).$$

This function is zero at the extremes and peaks in the middle of the range.

$$\text{High Membership Function: } \mu_{\text{High}}(x) = \max\left(0, \min\left(\frac{x-5}{5}, 1\right)\right).$$

This function is zero at the lower end of the range and increases linearly to one as x reaches its maximum value.

1.1.5. Fuzzy rule base

Fuzzy rules define the relationship between input and output fuzzy sets [15]. A representative rule in the present acoustic setting is:

IF sound level is High AND exposure duration is Long AND source–receiver distance is near THEN Noise-Risk Index is Critical

Where:

μ_L, μ_D, and μ_{ER} denote the membership functions for sound level, exposure duration, and source–receiver distance, respectively. μ_{RL} is the resulting membership function for the Noise-Risk Index.

1.1.6. Fuzzy inference

The fuzzy inference process combines the input membership values using a logical operator, typically the minimum (AND operation) [16]:

$$\mu_{\text{RL}}(\text{x}) = \min\left(\mu_{\text{MV}}(\text{x}), \mu_{\text{ID}}(\text{x}), \mu_{\text{ER}}(\text{x})\right).$$

This operation yields the degree of membership for the output fuzzy set based on the input conditions.

1.1.7. Defuzzification

To convert the fuzzy output back into a crisp value, the centroid (center-of-gravity) method is used [17, 18]: The min-max inference and centroid defuzzification expressions are standard Mamdani formulations [16–18].

$$RL_{\text{def}} = \frac{\sum\ (\mu_{\text{RL}}(x) \times x)}{\sum\ \mu_{\text{RL}}(x)}.$$

Where:

$R\ L_{def}$ is the defuzzified output value for the Noise-Risk Index.

x_i represents the discrete values over which the fuzzy set is defined.

1.2. Research gap and contributions

The research question is whether a classical harmonic representation and a transparent fuzzy decision layer can be combined in a single acoustics-oriented workflow without conflating their roles. The novelty emerges from combining (i) a practically stated Fourier–Dirichlet approximation viewpoint on sampled audio, (ii) an illustrative hyperbolic-series relationship that allows for compact analytical discussion, and (iii) Mamdani fuzzy model that translates uncertain acoustic measurements to interpretable classes of risk. Throughout the paper, the hyperbolic component is treated only as a schematic coefficient-pattern template and not as an alternative basis or new convergence result.

The paper focuses on the fuzzy acoustic module from an applied perspective. While the Fourier and hyperbolic sections serve as a signal-description background, uncertainty-aware risk interpretation across representative acoustics scenarios is the main engineering contribution.

1.3. Summary of contributions and organization

This study made four contributions. First, it reformulated the classical Fourier-Dirichlet perspective on sampled acoustic signals in a practically verifiable form. Second, it limited the hyperbolic part to a standardized coefficient-pattern template and not a separate basis equivalence. Third, it developed an interpretable Mamdani fuzzy system for acoustic noise-risk assessment utilising indicators such as L_{Aeq}, daily exposure time, and source-to-receiver distance. Fourth, it showed the fuzzy model qualitatively for 12 representative scenarios and compared its classes to a simple crisp screening baseline, achieving 10/12 class agreement and smoother behavior near decision boundaries.

The rest of the paper is structured as follows. The study objective is presented in Section 2. Mathematical background, and the limited hyperbolic-template comparison, are in Sections 3 and 4. Examples of signal approximation are in Sections 5–7. Section 8 elaborates the fuzzy acoustic risk model, and Sections 9 and 10 illustrate future work and conclusions.

2. Objective of the study

The study involves two related goals: It first proposes a compact Fourier–Dirichlet perspective on the approximation of periodic acoustic signals and on providing an interpretation for truncated harmonic sum convergence. At first, it proposes a Mamdani-type fuzzy inference system to reason uncertainty-aware acoustic noise-risk assessment based on sound level, exposure duration, and distance.

The articulation between the two segments is application-based: Fourier analysis describes the waveform content within measured acoustic signals, and fuzzy inference provides a “translation” from uncertain exposure descriptors to an operable risk category that informs sound & vibration practice.

3. Problem statement 1: Dirichlet conditions and hyperbolic-series relation

Consider a piecewise-continuous periodic function $f(x)$ on a finite interval that satisfies the Dirichlet conditions:

(i) Let f(x) be a piecewise continuous function on the interval of interest.

(ii) $f(x)$ has a Fourier series representation given by:

$$f(x) = \frac{a_0}{2} + \sum\nolimits_{n=1}^{\infty} \left(a_n cos(nx) + b_n sin(nx)\right),$$

where a_n and b_n are the Fourier coefficients.

(iii) Assume that the Dirichlet conditions are satisfied for $f(x)$, so the Fourier series converges in the classical pointwise sense on the interval.

We seek only a schematic coefficient-pattern comparison with the finite hyperbolic template:

$$H_{N(x)} = \Sigma_{\{n=1\}}^{\{N\}} c_n \;\; sinh(nx), \quad N < \infty.$$

Solution:

(i) Expression of f(x) using Fourier series: Given that f(x) has a Fourier series representation, write it in terms of cosine and sine functions:

$$f(x) = \frac{a_0}{2} + \sum\nolimits_{n=1}^{\infty} \left(a_n cos(nx) + b_n sin(nx)\right).$$

(ii) Dirichlet conditions: These conditions guarantee the standard convergence of the Fourier representation of f(x) on the interval.

(iii) Connection to hyperbolic template: Consider the following finite hyperbolic template:

$$H_{N(x)} = \; \Sigma_{\{n=1\}}^{\{N\}} c_n \, sinh(nx), \quad N < \infty.$$

(iv) Coefficient-pattern comparison: Since hyperbolic and trigonometric functions are different bases, we do not match term-by-term. The mere question is whether a given growth sequence c_n can approximate the oscillation pattern of some selected Fourier sine coefficients. $c_n \leftrightarrow b_n$ (comparison of coefficient magnitudes only). This establishes only an auxiliary comparison of coefficient sequences, hence not an equality between hyperbolic and trigonometric basis functions.

(v) The Fourier expansion is retained, where the approximation of $f(x)$ always remains the trigonometric Fourier series, in which only the hyperbolic template is used as a separate descriptor of selected weights.

$$f_{N(x)} = \frac{a_0}{2} \; + \; \Sigma_{n=1}^{N} \; \left[a_n \; cos(nx) + b_n \; sin(nx)\right].$$

In this limited sense, the hyperbolic template serves as compact bookkeeping for a chosen coefficient pattern. No independent hyperbolic convergence claim is made.

4. Problem statement 2: Electrical signal approximation under Dirichlet conditions

Signal modeling is a fundamental issue in electrical engineering. Let a continuous periodic signal be of the form V(t), where *t* is in [0, T], and T is the period of the original signal. This means expressing the signal in terms of Fourier expansion.

The signal V(t): The signal you have is known to you, and continuous on [0, T]. Its Fourier series representation is:

$$V(t) = \frac{a_0}{2} + \sum\nolimits_{n=1}^{\infty} \left(a_n cos\left(\frac{2\pi nt}{T}\right) + b_n sin\left(\frac{2\pi nt}{T}\right)\right) \ ,$$

where a_n and b_n are the Fourier coefficients.

Dirichlet conditions: The Dirichlet conditions can be checked for V(t) to verify the standard convergence of Fourier series.

Illustrative hyperbolic template: Consider the following finite hyperbolic template for the signal V(t):

$$H_{N(t)} = \Sigma_{n=1}^{N} \, c_n \, sinh(2\pi nt/T), \quad N < \infty.$$

4.1. Solution

Fourier series representation for V(t): The signal V(t) can be expressed in terms of its Fourier series.

Dirichlet conditions: Since the Dirichlet conditions are satisfied for V(t), then, accordingly, at the continuity points of an interval J ⊂ R1 it holds true that Fourier partial sums have a classical pointwise interpretation.

Hyperbolic template link: This is our comparison to a finite hyperbolic template of the Fourier representation:

$$H_{N(t)} = \Sigma_{n=1}^{N} \, c_n \, sinh(2\pi nt/T), \quad N < \infty.$$

Coefficient-pattern comparison: we compare the selected Fourier sine coefficients with those illustrative weights c_n; no term-by-term basis-to-identification is claimed [26,27].

The Fourier series thus continues to represent the signal V(t); the hyperbolic representation is just a companion expression that describes a selected sequence of weights.

Summary and ending remarks: We demonstrate that a chosen hyperbolic-weight sequence plays along nicely with the Fourier coefficients of an electrical signal; there is no new identity or basis equivalence here.

4.2. Real-world context

In any practical application, V(t) can be an electrical signal (e.g., an AC voltage waveform), and Fourier series is still a standard technique to study such signals. The hyperbolic-series relation is included here for completeness as an additional analytical form for some coefficient patterns.

The precise form depends on the particular signal and its Fourier coefficients. Thus, this example should be considered as a line of reasoning and not a universal property for any arbitrary electrical waveforms.

5. Case study: Audio signal approximation

Example problem context: Signal approximation is at the core of audio engineering and covers a wide range of applications such as sound synthesis, compression, and harmonic analysis. Let us take the example of a simple, periodic audio waveform from a piano note.

5.1. Interpretation of noise risk using a fuzzy inference system (uncertainty-aware layer)

In this work, a Mamdani-type fuzzy inference system (FIS) using measurable acoustic and contextual variables is introduced to express uncertainty in the practical assessment of noise exposure. Instead of relying solely on crisp thresholds, the idea is to translate vague or fuzzy conditions into a linguistic Noise-Risk Index. This design follows recent fuzzy-acoustic studies related to urban noise indexes and subjective noise annoyance [13,14,28].

Inputs: $L_{Aeq}(dBA)$: A-weighted equivalent continuous sound level.

T (hours/day): daily exposure duration: $D(m)$: source–receiver distance.

Output: Noise-Risk Index (linguistic): $\{$Safe, Caution, High, Critical$\}$.

All inputs are described by three fuzzy sets, which can be trapezoidal or triangular membership functions. L_{Aeq} Low is therefore centered below approximately 70 dBA, L_{Aeq} Medium covers the intermediate region of overlap around 65–85 dBA, while L_{Aeq} High starts above around 80 dBA, so that transitions are gradual with respect to both measurement uncertainty and contextual variation.

Inference rules:

- If L_{Aeq} is High and T is Long then Risk is Critical.
- If L_{Aeq} is Medium and T is Long then Risk is High.
- If L_{Aeq} is Medium and T is Short and D is Far then Risk is Caution.
- If L_{Aeq} is Low then Risk is Safe.

Defuzzification is performed using the centroid method to obtain a scalar risk score that is reported together with the linguistic class.

Given information:

- The audio signal *x(t)* representing the musical note has a fundamental frequency of 440 Hz (A4 note), and its period T is 1/440 seconds.
- We aim to approximate *x(t)* using its Fourier series expansion.

5.2. Solution steps

The workflow used in this illustrative example is summarized in **Figure 1**.

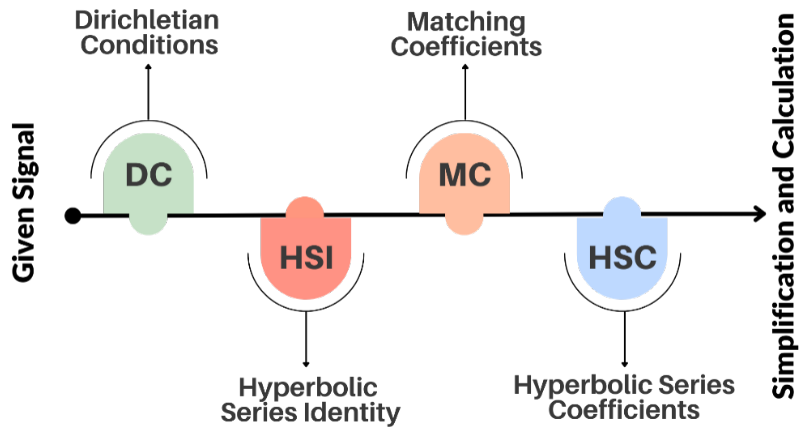

Figure 1. Workflow used to solve the illustrative audio approximation problem.

i. Given signal: The audio signal *x(t)* can be represented by its Fourier series expansion:

$$V(t) = \frac{a_0}{2} + \sum_{n=1}^{\infty} \left(a_n cos(2\pi n f t) + b_n sin(2\pi n f t)\right),$$

where f_0 is the fundamental frequency (440 Hz in this case) and a_n and b_n are the Fourier coefficients.

ii. Dirichlet conditions: Assuming that the Dirichlet conditions are satisfied for *x(t)*, we proceed with the Fourier series representation.

iii. Illustrative hyperbolic template: We examine the following finite hyperbolic template:

$$H_{N(t)} = \Sigma_{n=1}^{N} c_n \, sinh(2\pi n \, f_0 \, t).$$

iv. Coefficient-pattern comparison: For this illustrative case, assume a simplified weight sequence $\{c_n\}$ for the retained terms.

v. Fourier approximation retained: the waveform approximation itself remains the Fourier series truncated to the retained harmonics:

$$x_{N(t)} = \frac{a_0}{2} + \Sigma_{n=1}^{N} \left[a_n \, cos\,(2\pi n \, f_0 \, t) + \, b_n \, sin\,(2\pi n \, f_0 \, t)\right].$$

vi. Parameter specification: For the A4 note, $f_0 \; = \; 440$ Hz and T = 1/440 s; the hyperbolic template is kept separate from the Fourier reconstruction.

$$H_{N(t)} = \Sigma_{n=1}^{N} c_n \, sinh(2\pi n \cdot 440 \, t).$$

The regularity of $x(t)$ determines whether the Fourier series converges at a point. If $x(t)$ fulfills Dirichlet's criteria, the partial sums converge to $x(t)$ at vicinity points and also to the value of the jump in discontinuities; Gibbs oscillation remains around jumps, which is relevant for clipped or enriched audio waveforms.

In this simple example, hyperbolic expression is merely an auxiliary template for coefficient-pattern discussion; the underlying observations are of course still subject to numerical coefficient fits and finite-record treatment.

6. Example: Finite hyperbolic-template terms

We consider a representative periodic audio waveform corresponding to a musical tone under this study. As a simple reference, an A4 tone has a fundamental frequency f_0 = 440 Hz, hence the period is:

$$T = \frac{1}{f_0} \approx 2.273 \times 10^{-3} \text{ s} .$$

The goal is to reconstruct the waveform with partial Fourier sums and assess reconstruction error as a function of harmonic number. The former demonstrates convergence behavior in practice and clarifies the role of Dirichlet conditions for audio reconstruction from finite sets of harmonic content.

For numerical demonstration, the coefficients a_n and b_n are calculated from a chosen waveform using either (i) analytical expressions for a standard waveform (e.g., square, or sawtooth) or (ii) discrete estimation based on the sampled signal $x[k]$ over one period. We thus simulate a true measurement workflow; in this paper, we use discrete coefficient estimation from uniformly sampled data. The sum over N_h harmonics reads as:

$$x_{N_h}(t) = \frac{a_0}{2} + \sum\nolimits_{n=1}^{N_h} \left[a_n \cos\left(n\omega_0 t\right) + b_n \sin\left(n\omega_0 t\right)\right] .$$

Now, reconstruction quality is quantified using RMSE and spectral-magnitude deviation over the harmonics retained.

For the finite hyperbolic template:

$$H_{N(t)} = \Sigma_{n=1}^{N} \, c_n \; sinh(2\pi n \; f_0 \; t),$$

where f = 440 Hz (frequency of the A4 note) and t is the time variable.

We list the first few template terms:

For n = 1: $c_1 \; sinh(880\pi t)$;

For n = 2: $c_2 \; sinh(1,760\pi t)$;

For n = 3: $c_3 \; sinh(2,640\pi t)$.

Summing the first three template terms:

$$H_{3(t)} = c_1 sinh(880\pi t) + c_2 sinh(1,760\pi t) + c_3 sinh(2,640\pi t).$$

There is no comparison with a separate closed-form right-hand side; the expression only serves to illustrate the first few hyperbolic terms.

It is worth mentioning that these terms are merely a finite illustrative template. They do not suggest convergence to an easily understood closed formula, and any practical application would still require the specification of individual coefficients with numerical evaluation. But in practice, we would treat any such finite hyperbolic template numerically.

7. Case study: Electrical signal approximation using Fourier series and hyperbolic functions

7.1. Purpose

The case study demonstrates the Fourier series and an illustrative hyperbolic-weight template-based approach to approximate a simple electrical signal. The study of Fourier expansion for a periodic signal is followed, keeping the hyperbolic expression only as an adjunctive descriptor of certain coefficient patterns.

7.2. Background

Fourier series decompose periodic signals into sums of sinusoidal elements. In this scheme, Dirichlet conditions ensure ordinary convergence behavior (which is possible only for specific weights), and the hyperbolic template below represents a schematic analytical counterpart.

7.3. Problem context

Consider an electrical signal $V(t)$, which is a continuous periodic signal with a fundamental frequency $f_0 = 50$ Hz. The period of the signal is $T = \frac{1}{f_0} = 0.02$ seconds. The signal can be represented as:

$$V(t) = a_0 + \sum\nolimits_{n=1}^{\infty} \left(a_n \cos\left(\frac{2\pi nt}{T}\right) + b_n \sin\left(\frac{2\pi nt}{T}\right)\right).$$

Given signal: Let the signal V(t) be defined as follows:

$$V(t) = \begin{cases} 0 & \text{for } 0 \le t < T/2 \\ 10\text{ V} & \text{for } T/2 \le t < T \end{cases}.$$

This signal represents a simple square wave with a peak amplitude of 10 V.

7.4. Steps

Step 1: Fourier series representation

The Fourier coefficients a_n and b_n for the signal $V(t)$ are calculated as follows: This square-wave coefficient calculation is classical and is included here only for illustration [20].

$$\begin{aligned} a_0 &= \tfrac{2}{T}\int_0^T V(t)dt, \\ a_n &= \tfrac{2}{T}\int_0^T V(t)\cos\left(\tfrac{2\pi nt}{T}\right)dt, \\ b_n &= \tfrac{2}{T}\int_0^T V(t)\sin\left(\tfrac{2\pi nt}{T}\right)dt. \end{aligned}$$

Calculation:

(i) For a_0:

$$\begin{aligned} a_0 &= \tfrac{2}{0.02}\left(\int_0^{0.01} 0dt + \int_{0.01}^{0.02} 10dt\right) \\ a_0 &= \tfrac{2}{0.02}(0 + 10 \times 0.01) = 100\text{ V}. \end{aligned},$$

(ii) For a_n: For the centered odd square-wave representation, $a_n = 0$ for all n.

(iii) For b_n:

$$b_n = \frac{2}{0.02}\int_{0.01}^{0.02} 10\sin\left(\frac{2\pi nt}{0.02}\right)dt.$$

Performing the integration:

$$\begin{gathered} b_n = \tfrac{100}{\pi n}\left[-\cos\left(\tfrac{2\pi nt}{0.02}\right)\right]_{0.01}^{0.02} \\ b_n = \tfrac{100}{\pi n}\left(-\cos(2\pi n)+\cos(\pi n)\right) \end{gathered}.$$

For odd n:

$$b_n = \frac{200}{\pi n}.$$

For even n:

$$b_n = 0.$$

Thus, the Fourier series for $V(t)$ is:

$$V(t) = \frac{100}{2} + \sum\nolimits_{n=1,3,5,...}^{\infty} \frac{200}{\pi n}\sin\left(\frac{2\pi nt}{0.02}\right).$$

Step 2: Dirichlet conditions and boundary behaviour

In this context, the relevant requirement is the Dirichlet conditions for Fourier convergence rather than the PDE Dirichlet problem. For the square wave, the partial sums converge to the signal at continuity points and to the midpoint of the jump at discontinuities.

Since $V(t)$ is piecewise constant with a jump at $t = T/2$, the Dirichlet conditions are satisfied.

Step 3: Hyperbolic-weight template

We investigate relating the Fourier coefficients to a finite hyperbolic template. Consider

$$H_{N(t)} = \Sigma_{n=1}^{N}\, c_n\, sinh(2\pi nt/T).$$

For the same signal *V(t)* we compare a selection of Fourier coefficients with the illustrative hyperbolic weights c_n which serve here as a formal analytic device for discussing selected coefficient patterns rather than as a universal identity.

Step 4: Real-world application—signal approximation

Through the Fourier series expansion, *V(t)* can be approximated by truncating to a finite number of terms:

$$V(t) \approx \frac{100}{2} + \frac{200}{\pi}\left(\sin(100\pi t) + \frac{1}{3}\sin(300\pi t) + \frac{1}{5}\sin(500\pi t)\right).$$

For many applications, the square wave can be approximated as a sum of these sinusoidal components.

Step 5: Numerical calculation and plotting

The resulting approximation of this study, shown in **Figure 2**, uses the first few nonzero harmonics. The below **Figure 2** presents the Fourier-series approximation of the square-wave signal, including the discontinuity at t = T/2.

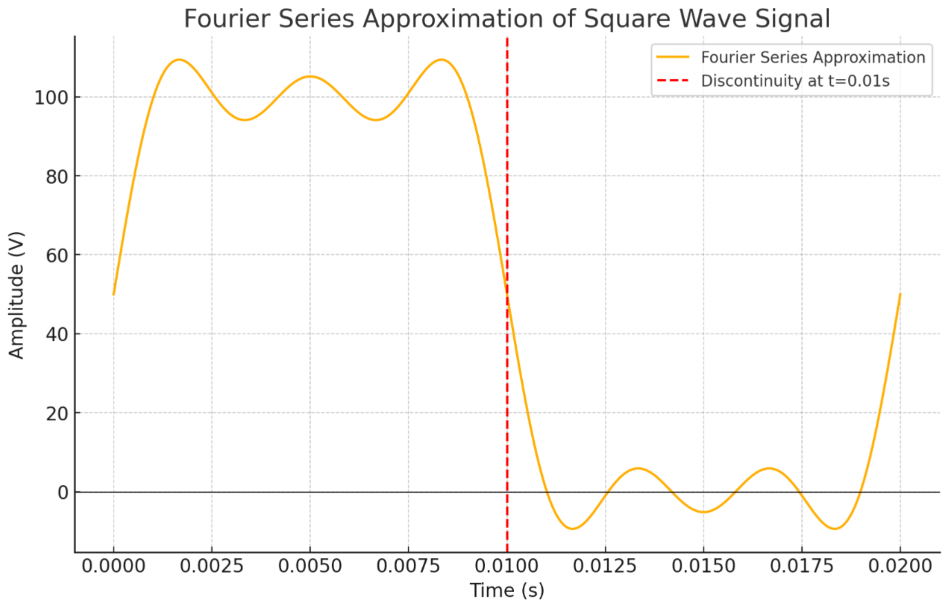

Figure 2. The first three odd harmonics of the Fourier series for *V(t)* and the resulting approximation, plotted as amplitude (*V*) versus time (*s*).

As shown in this case study, Fourier series offer a readily interpretable harmonic approximation to a signal-square-wave type electrical signal, and the hyperbolic-series relation can encompass an auxiliary analytical description of some particular represented coefficient structures.

The same analytical perspective may also be generalized for advanced signals as long as the assumptions about periodicity and convergence are clearly stated when needed, and when its interpretation has an association with the physical signal being studied.

8. Case study: Fuzzy logic-based acoustic noise exposure risk assessment

8.1. Motivation and problem statement

In actual sound and noise engineering (sensor-based sound monitoring), the risk of exposure is often assessed on deterministic thresholds, while recorded values are not only time-variant (e.g., operating conditions: traffic load, machine duty cycle, wind reflections) but vary among people and across work shifts—human muscular fatigue can cause an individual to behave as a passive sensor. In order to enable solid decision-making in conditions of such imprecision, this case study creates a Mamdani-type fuzzy inference system (FIS) that classifies the daily risk of noise exposure based on both standard acoustic descriptors and workplace context. These have still been described as being similar motivations for other recent fuzzy-acoustic studies in urban noise indexes and subjective noise annoyance [13,14,29].

8.2. Input-output variables and parameters

We introduce a three-input fuzzy model typically applied in occupational/ environmental acoustics:

Inputs:

- A-weighted equivalent continuous level L_{Aeq} (dBA);
- Daily exposure duration T (hours/day);
- Source–receiver distance D (m) (captures geometric attenuation/proximity; can be omitted if not available).

Output:

Exposure risk index R on [0,100] with linguistic levels: Safe (S), Caution (C), High (H), Critical (CR)

Common measurement uncertainty (to be interpreted, not compulsory):

Short-term variability can be due to instrument tolerance as well as variations in reading. In order to reflect this, results can be given using scenario ranges, while fuzzy logic accommodates imprecision by nature via overlapping memberships.

8.3. Membership function design

Triangular and trapezoidal functions are used for simplicity and interpretability.

The discourse universes were initialized from practical occupational and shelter screening bands: levels below ∼70 dBA represent low-risk indoor/edge conditions, the 80–85 dBA region indicates a protective transition band of common use in occupational assessment, and values around or above 95 dBA indicate clearly severe cases for screening purposes. The current boundaries, therefore, are illustrative rather than arbitrary; they have been determined to be comparable to conventional exposure-assessment practice and should be readjusted according to local regulations, ISO 1999-based hearing-risk estimation, or site-specific (ISO 1999) surveys [6,9,30,31].

8.3.1. Memberships for L_{Aeq} (dBA)

Universe: $L_{Aeq} \in [55, 105]$

- Low (L): trapezoid [55, 55, 60, 70];
- Moderate (M): triangle [65, 75, 85];
- High (H): triangle [80, 90, 98];
- Very High (VH): trapezoid [95, 100, 105, 105].

These boundaries are illustrative and can be adjusted to match local regulations or institutional exposure guidelines.

8.3.2. Memberships for T (hours/day)

Universe: $T \in [0,10]$

- Short (S): trapezoid [0, 0, 1, 3];
- Medium (MD): triangle [2,4,6];
- Long (L): triangle [5, 7, 9];
- Very Long (VL): trapezoid [8, 9, 10, 10].

8.3.3. Memberships for D (m)

Universe: $D \in [1,50]$

- Near (N): trapezoid [1, 1, 3, 8];

- Mid (MID): triangle [6, 15, 25];
- Far (F): trapezoid [20,35,50,50].

8.3.4. Output memberships for risk R

- Safe (S): trapezoid [0, 0, 15, 30];
- Caution (C): triangle [20, 40, 55];
- High (H): triangle [50, 70, 85];
- Critical (CR): trapezoid [80, 90, 100, 100].

The human-defined fuzzy membership functions for L_{Aeq}, exposure duration T, and source–receiver distance D are depicted in **Figure 3**, which gives the linguistic partitions utilized by Mamdani inference system.

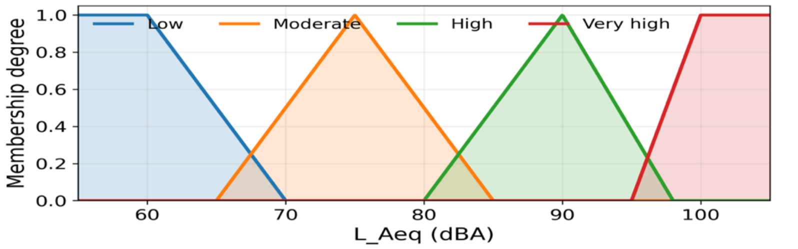

(a) A-weighted equivalent sound level

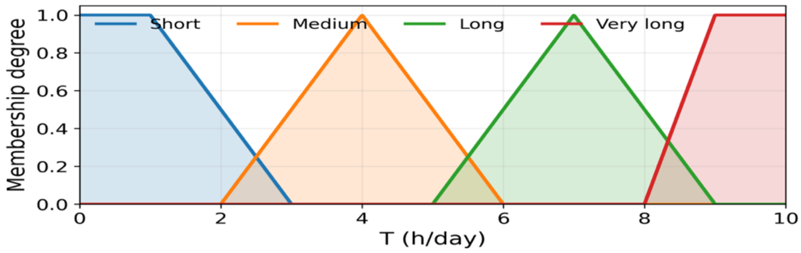

(b) Daily exposure duration

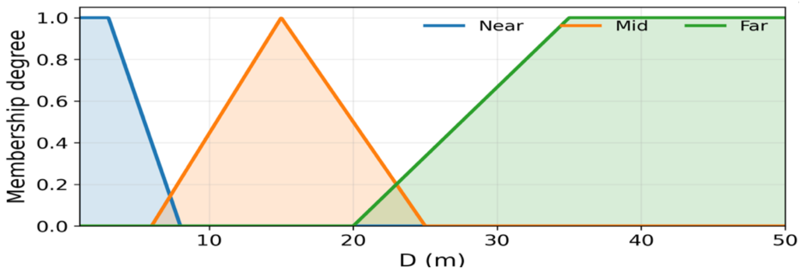

(c) Source-receiver distance

Figure 3. Fuzzy membership functions used for acoustic noise exposure risk assessment.

(a) Input fuzzy sets for the A-weighted equivalent sound level L_{Aeq} (dBA), defined as Low, Moderate, High, and Very High.
(b) Input fuzzy sets for daily exposure time T (h/day), defined as Short, Medium, Long, and Very Long.
(c) Input fuzzy sets for source-receiver distance D(m), defined as Near, Mid, and Far.

These overlapping membership functions form the input layer of the Mamdani fuzzy inference system and enable smooth risk transitions under measurement variability and uncertain exposure conditions.

8.4. Fuzzy rule base (Mamdani)

These simple rules are consistent with engineering intuition: risk increases with SPL, and with exposure time, and distance is a proxy for greater effective exposure.

Core rules (12 representative rules):

(1) IF L_{Aeq} is Low → Risk is Safe;
(2) IF L_{Aeq} is Moderate AND T is Short → Risk is Caution;
(3) IF L_{Aeq} is Moderate AND T is Medium → Risk is Caution;
(4) IF L_{Aeq} is Moderate AND T is Long → Risk is High;
(5) IF L_{Aeq} is High AND T is Short → Risk is High;
(6) IF L_{Aeq} is High AND T is Medium → Risk is High;
(7) IF L_{Aeq} is High AND T is Long → Risk is Critical;
(8) IF L_{Aeq} is Very High → Risk is Critical.

Distance modulation is included to improve engineering realism:

(9) IF L_{Aeq} is Moderate AND T is Medium AND D is Near → Risk is High;
(10) IF L_{Aeq} is High AND T is Medium AND D is Near → Risk is Critical;
(11) IF L_{Aeq} is High AND T is Short AND D is Far → Risk is Caution;
(12) IF L_{Aeq} is Moderate AND T is Long AND D is Far → Risk is Caution.

Rules 11–12 capture the reduction in effective exposure associated with greater distance. If a simpler model is preferred, the distance rules may be omitted, and the system may be restricted to L_{Aeq} and T.

8.5. Inference and defuzzification

We use the standard Mamdani inference:

- AND operator: min;
- OR operator: max;
- Implication: min;
- Aggregation: max;
- Defuzzification: centroid.

$$R^* = \frac{\int_0^{100} r\mu_R(r)dr}{\int_0^{100} \mu_R(r)dr}.$$

Risk category can be assigned by the maximum membership of the output set or by numeric thresholds, e.g.,

- $R^* < 30$: Safe;
- $30 \leq R^* < 55$: Caution;
- $55 \leq R^* < 80$: High;
- $R^* \geq 80$: Critical.

8.6. Scenario dataset and results

To demonstrate usability, we evaluate 12 representative scenarios covering three common acoustics contexts: transportation noise, workshop/industrial exposure, and public-address or event amplification. These are constructed scenarios intended to test interpretability and boundary behavior; they are not presented as substitutes for field measurements (**Table 1**).

Table 1. Exposure scenarios and fuzzy risk outputs.

Scenario	Context (example)	L_{Aeq} (dBA)	T (h/day)	D (m)	Fuzzy Risk R* (0–100)	Category	Suggested action
S1	Quiet office/library edge	62	6	10	22	Safe	No action; periodic check
S2	Moderate traffic façade	74	4	15	43	Caution	Monitor; improve sealing
S3	School roadside (peak hours)	79	6	8	56	High	Schedule control + barrier feasibility
S4	Light workshop tools	82	2	6	60	High	PPE optional; task rotation
S5	Busy junction vendor	85	8	5	78	High	PPE recommended; exposure reduction
S6	Generator room corridor	90	4	4	86	Critical	PPE + engineering controls
S7	Road maintenance activity	92	2	10	73	High	PPE + time limits
S8	Diesel bus bay	95	6	6	92	Critical	Immediate mitigation; administrative control
S9	Factory compressor area	88	7	3	90	Critical	Enclosure/absorption + PPE
S10	Public event loudspeaker	98	1.5	12	82	Critical	Distance zoning + level control
S11	Residential (night) near highway	76	8	25	45	Caution	Window improvements; barrier study
S12	Classroom internal fan noise	68	5	2	30	Caution	Maintenance; vibration isolation

For a comparative marker, the same 12 scenarios were also evaluated against a simple crisp rule set based on the exposure bands: Safe < 70 dBA, Caution 70–79 dBA, High 80–89 dBA, Critical ≥ 90 dBA—adjusted upward one class for long-near cases (T ≥ 6 h/day and D ≤ 8 m), downward for short-far cases (T ≤ 2 h/day and D ≥ 10 m) and establishing minimum Caution class dispositions for low-level but very near cases. In 10 of the 12 scenarios, this crisp screen concurred with the fuzzy category. Both disagreements occurred at borders (S5 and S10) where the fuzzy overlaps were explicitly designed to alleviate sharp changes between classes. Therefore, this comparison should be seen as a sanity check rather than external validation.

Interpretation of outcomes (engineering view):

- Scenarios approaching or exceeding 90 dBA L_{Aeq} generally map to Critical (S6, S8, S9) at long exposure times and/or close receiver proximity.
- Moderate sound levels are generally rated as Caution or High, depending strongly on duration and distance (for example, S2 versus S3).
- Short-duration high noise can be High rather than Critical, acknowledging that exposure duration is still a decisive factor in practical assessment (e.g., S7).

(NOTE: If your measured L_{Aeq} ranges are within ±2 dB, you can repeat each scenario at L_{Aeq} − 2 dB and L_{Aeq} + 2 dB to report a risk interval for R.)

The outputs of the fuzzy inference are visually summarized in **Figure 4**, which displays the defuzzified risk index R as a function of L_{Aeq} and T (h/day). The surface depicts the increase in risk nonlinearly with both levels and durations, whereas the distance-to-source condition extrapolates the surface upward for closer proximity. Thus, the figure provides a visual representation of the decision regions of the Safe, Caution, High, and Critical classifications through the Mamdani system proposed.

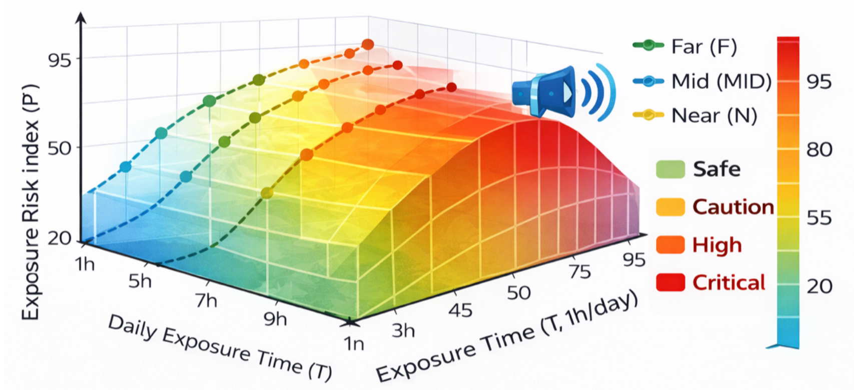

Figure 4. Fuzzy risk surface for acoustic noise exposure assessment.

8.7. Practical mitigation mapping (SV-friendly)

Linking the risk index to controllable acoustics practice, recommended controls can be described as:

Chose (0–30): intermittent checkups; preventive maintenance.

Caution (30–55): administrative controls; minor absorptive treatments; resealing; enforce quiet-time scheduling.

High (55–80): PPE recommended; decrease exposure time; consider shielding barriers/enclosures; maintenance sourcing, structure-borne contributions vibration isolation.

Critical (80–100): immediate mitigation priority—engineering controls (enclosures/barriers), strict exposure limits, and a verified hearing conservation plan.

8.8. Discussion: Why fuzzy logic helps in acoustic exposure assessment

This case study demonstrates that fuzzy inference offers:

- Fluent risk transitions, without creating hard limits at specific dBA values.
- Makes a single interpretable index across heterogeneous information (level, time, and proximity)
- Overlapping memberships handle time-varying levels and uncertain exposure patterns, which brings robustness to variability.
- Risk label + action is a form of decision support with high communicability to non-specialists.
- The output of scenarios in **Table 1** showed monotonic behavior with the closest exposure descriptors. For example, a transition from S2 (74 dBA, 4 h/day, 15 m) to S3 (79 dBA, 6 h/day, 8 m) led to an increase in the score from 43 to 56 and a change in the class from Caution to High—an indication that simultaneous increases in level, duration, and proximity simultaneously activate multiple rules. Similarly, S6, S8, and S9 were also part of the Critical zone as very high level, sustained duration, or very short distance fired the upper output memberships with high firing strength.
- These compare in crisp-baselines, makes the value of fuzzy formulation that more clear. The agreement in 10 of 12 scenarios suggests the rule base largely reproduces standard screening expectations, while the two discrepancies

underscore why fuzzy overlap is helpful near thresholds. S5 was High, rather than Critical due to the lack of complete domination by any single variable in the inference (while S10 remained Critical as a very high level activated substantial upper-risk despite the short exposure time). This more smoothly behaved option is desirable when measurements vary by a few decibels or when contextual details are vague.

- While the outcomes should still be viewed in light of their existing limitations: the scenarios are merely demonstrative and no direct input from the Fourier stage to a fuzzy engine was made yet. In the present paper, the relationship is not feature-coupled but sequential, such that harmonic analysis provides a reliable description of measured waveforms while interpretive components in the fuzzy layer related to reduced exposure descriptors characterize L_{Aeq}, T, and D; nevertheless, this ordering of lower- and higher-risk scenarios aligns well with recent findings from field-based occupational studies, which indicate increased health burdens after repeated exposures across widely applicable protective bands around 85 dBA [9,32]. A more tightly integrated use of spectral descriptors (e.g., tonal prominence, band-limited energy, or impulsiveness) is still a future direction.

8.9. Reproducibility notes

This model can be replicated with any fuzzy toolbox (MATLAB Fuzzy Logic Toolbox/Python scikit-fuzzy). These all together (Subsection 8.3 for membership parameters and Subsection 8.4 for rule base) combine to fully specify the inference engine. The scalar risk index R^* is obtained using centroid defuzzification (Subsection 8.5).

9. Scope for future work

According to this study, future work will focus on three specific extensions of the present study, summarized in **Figure 5**. First, the Fourier component will be extended to windowed or short-time analysis for nonstationary audio so that convergence can be interpreted locally in time.

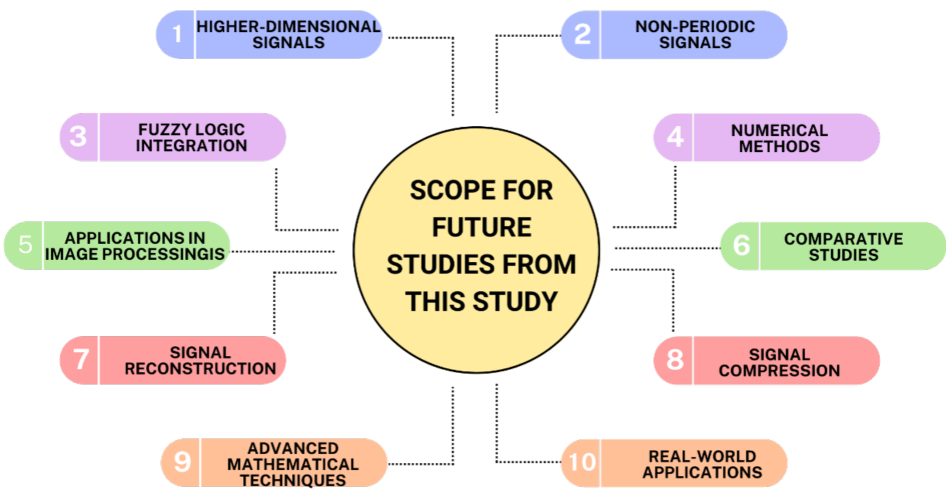

Figure 5. Specific future directions of the proposed acoustics framework.

Second, the fuzzy module will be calibrated using repeated field measurements and expert judgment so that the membership boundaries for sound level, exposure duration, and distance are data-informed rather than purely illustrative.

Third, the integrated framework will be validated using measured datasets collected in traffic corridors, workshops, and amplified public-event settings in comparison to thresholds-based screening techniques. A further priority is to feed spectral descriptors extracted from the signal-analysis stage directly into the fuzzy model so that the two layers become operationally coupled rather than only sequential.

Such steps would enhance both the interpretational signalling to signal analysis and mean that the proposed uncertainty-aware acoustic assessment was practically reliable.

10. Conclusion

This study integrated classical Fourier-Dirichlet periodic descriptors for acoustic signals and an interpretable Mamdani fuzzy approach to screen for noise risk in their recordings. It reformulated the Fourier conditions in an easily verifiable form suitable for sampled outcomes; it restricted hyperbolic to be replaced by a template of schematic coefficient patterns; and it powered the fuzzy system, applied on 12 typical exposure scenarios. The derived Noise-Risk Index was within the range of 22–92 for each class, while the treaded crisp-baseline comparison showed a 10/12 class agreement and an overall smooth relation sustained by the fuzzy model in cases close to extremes.

Future work should (i) cross-calibrate the membership boundaries and rule base with repeated field measurements and relevant regulatory/ISO guidance, and (ii) apply the framework to measured datasets from traffic/workshop/generator-room environments so as to report systematic comparisons against classical threshold-based assessments. A second priority is to more closely tie the signal-analysis stage to that of decision by making use of spectral descriptors, such as tonal prominence, impulsiveness, or band-limited energy, as additional fuzzy inputs.

In that state, the framework transparently bridged signal description and uncertainty-aware exposure screening while clarifying that the current coupling was sequential rather than full integration.

Author contributions: Conceptualization, YN and AV; methodology, YN; software, YN and SEH; validation, AV, ZPM and CWO; formal analysis, YN; investigation, YN and MA; resources, AV and MA; data curation, YN; writing—original draft preparation, YN; writing—review and editing, AV, SEH, ZPM, CWO and MA; visualization, YN and SEH; supervision, AV; project administration, YN and AV. All authors have read and agreed to the published version of the manuscript.

Funding: This work was not supported by specific grants from funders in the public, commercial, or not-for-profit sectors.

Institutional review board statement: Not applicable. This study did not involve human participants or animals.

Informed consent statement: Not applicable. This study did not involve human participants.

Data availability statement: No new experimental datasets were generated. All constructed scenarios and numerical values supporting the reported results are contained within the article.

Conflict of interest: The authors declare that there is no conflict of interest.

AI use statement: The authors used ChatGPT (OpenAI) for language refinement only while preparing this manuscript. AI tools were not used to analyse and interpret data or to generate scientific content. All output was reviewed for accuracy and edited by authors. The authors are responsible for the work's integrity and accuracy.

References

1. Khan D, Burdzik R. Measurement and analysis of transport noise and vibration: A review of techniques, case studies, and future directions. Measurement. 2023; 220: 113354. doi: 10.1016/j.measurement.2023.113354
2. Alharbi F, Luo S, Zhang H, et al. A Brief Review of Acoustic and Vibration Signal-Based Fault Detection for Belt Conveyor Idlers Using Machine Learning Models. Sensors. 2023; 23(4): 1902. doi: 10.3390/s23041902
3. Nawrocki W, Stryjski R, Kostrzewski M, et al. Application of the vibro-acoustic signal to evaluate wear in the spindle bearings of machining centres. In-service diagnostics in the automotive industry. Journal of Manufacturing Processes. 2023; 92: 165–178. doi: 10.1016/j.jmapro.2023.02.036
4. Wang X, Mao D, Li X. Bearing fault diagnosis based on vibro-acoustic data fusion and 1D-CNN network. Measurement. 2021; 173: 108518. doi: 10.1016/j.measurement.2020.108518
5. Tran T, Pham NT, Lundgren J. A deep learning approach for detecting drill bit failures from a small sound dataset. Scientific Reports. 2022; 12(1): 9623. doi: 10.1038/s41598-022-13237-7
6. Batko W, Radziszewski L, Bąkowski A. A Scalar Measure of Acoustic Hazard Assessment. Archives of Acoustics. 2024; 299–306. doi: 10.24425/aoa.2024.148793
7. Morillas JMB, González DM, Vílchez-Gómez R, et al. Estimation of the Occurrence and Significance of Noise Effects on Pedestrians Using Acoustic Variables Related to Sound Energy in Urban Environments. Applied Sciences. 2024; 14(23): 11212. doi: 10.3390/app142311212
8. Tsaligopoulos A, Aletta F, Maracchini G, et al. Rethinking environmental noise assessment through a noise footprint framework. Noise Mapping. 2025; 12(1): 20250019. doi: 10.1515/noise-2025-0019
9. Torres-Cobo L, Alcázar-Espinoza J, Vinueza-Morales M, et al. Occupational noise in the university setting: dosimetric assessment and strategies for exposure reduction. Frontiers in Public Health. 2025; 13: 1581677. doi: 10.3389/fpubh.2025.1581677
10. Asensio C, Pavón I, De Arcas G. A methodological framework for urban noise exposure assessment exploiting citizen itineraries and environmental noise maps. Applied Acoustics. 2026; 242: 111114. doi: 10.1016/j.apacoust.2025.111114
11. Ranpise RB, Tandel BN. Urban road traffic noise monitoring, mapping, modelling, and mitigation: A thematic review. Noise Mapping. 2022; 9(1): 48–66. doi: 10.1515/noise-2022-0004
12. Weidenfeld S, Sanok S, Fimmers R, et al. Short-Term Annoyance Due to Night-Time Road, Railway, and Air Traffic Noise: Role of the Noise Source, the Acoustical Metric, and Non-Acoustical Factors. International Journal of Environmental Research and Public Health. 2021; 18(9): 4647. doi: 10.3390/ijerph18094647
13. Fernández LPS. Environmental noise indicators and acoustic indexes based on fuzzy modelling for urban spaces. Ecological Indicators. 2021; 126: 107631. doi: 10.1016/j.ecolind.2021.107631
14. Fernandez-Prieto JA, Canada-Bago J, Birkel U. A Fuzzy Rule-Based System to Infer Subjective Noise Annoyance Using an Experimental Wireless Acoustic Sensor Network. Smart Cities. 2022; 5(4): 1574–1589. doi: 10.3390/smartcities5040080
15. Zadeh LA. Fuzzy sets. Information and Control. 1965; 8(3): 338–353. doi: 10.1016/S0019-9958(65)90241-X
16. Mamdani EH, Assilian S. An experiment in linguistic synthesis with a fuzzy logic controller. International Journal of Man-Machine Studies. 1975; 7(1): 1–13. doi: 10.1016/S0020-7373(75)80002-2

17. Ross TJ. Fuzzy Logic with Engineering Applications, 2nd ed. John Wiley & Sons; 2004.
18. Cox E. The Fuzzy Systems Handbook: A Practitioner's Guide to Building, Using, Maintaining Fuzzy Systems. AP Professional; 1994.
19. Courant R, Hilbert D. Methods of Mathematical Physics. Wiley; 1989. doi: 10.1002/9783527617210
20. Bracewell RN. The Fourier Transform and Its Applications, 3rd ed. McGraw-Hill; 2000.
21. Luenberger DG. Optimization by Vector Space Methods. Wiley; 2015.
22. Strang G. Introduction to Applied Mathematics. Wellesley-Cambridge Press; 1993.
23. Folland GB. Real Analysis: Modern Techniques and Their Applications, 2nd ed. John Wiley & Sons; 1999.
24. Rudin W. Principles of Mathematical Analysis, 3rd ed. McGraw-Hill; 2006.
25. Goodman R, Wallach NR. Representations and Invariants of the Classical Groups. Cambridge University Press; 1998.
26. Press WH, Teukolsky SA, Vetterling WT, Flannery BP. Numerical Recipes: The Art of Scientific Computing, 3rd ed. Cambridge University Press; 2007.
27. Rao SS. Vibration of Continuous Systems, 1st ed. Wiley; 2019. doi: 10.1002/9781119424284
28. Yadav M, Tandel B. Work Efficiency Prediction of Persons Working in Traffic Noise Environment Using Adaptive Neuro Fuzzy Inference System (ANFIS) Models. Archives of Acoustics. 2021; 677–683. doi: 10.24425/aoa.2021.139644
29. Mahapatra TK, Satapathy S, Panda SK. Evaluation and prediction of impact of noise on a worker in noisy environment by using ANFIS model. International Journal of System Assurance Engineering and Management. 2024; 15(3): 1172–1182. doi: 10.1007/s13198-023-02198-3
30. International Organization for Standardization. ISO 1999:2013: Acoustics—Estimation of Noise-Induced Hearing Loss. International Organization for Standardization; 2013. Available online: https://www.iso.org/standard/45103.html
31. Sahu AK, Nayak SK, Mohanty CR, et al. Traffic Noise and its Impact on Wellness of the Residents in Sambalpur City – a Critical Analysis. Archives of Acoustics. 2021; 353–363. doi: 10.24425/aoa.2021.136588
32. Cudjoe FA, Opoku DA, Ayisi-Boateng NK, et al. Health effects of occupational noise exposure on heavy-duty equipment operators and exposed workers in a mining firm in Ghana. PLOS One. 2025; 20(9): e0332600. doi: 10.1371/journal.pone.0332600